Common Crystalline and Magnetic Structure of Superconducting $A_2Fe_4Se_5$ (A = K, Rb, Cs, Tl) Single Crystals Measured Using Neutron Diffraction

F. Ye,[1] S. Chi,[1] Wei Bao,[2,*] X. F. Wang,[3] J. J. Ying,[3] X. H. Chen,[3] H. D. Wang,[4] C. H. Dong,[4] and Minghu Fang[4]

[1]*Neutron Scattering Science Division, Oak Ridge National Laboratory, Oak Ridge, Tennessee 37831, USA*

[2]*Department of Physics, Renmin University of China, Beijing 100872, China*

[3]*Hefei National Laboratory for Physical Science at Microscale and Department of Physics, University of Science and Technology of China, Hefei, Anhui 230026, China*

[4]*Department of Physics, Zhejiang University, Hangzhou 310027, China*

(Received 14 February 2011; published 19 September 2011)

Single-crystal neutron diffraction studies on superconductors $A_2Fe_4Se_5$, where A = Rb, Cs, (Tl, Rb), and (Tl, K) ($T_c \sim 30$ K), uncover the same Fe vacancy ordered crystal structure and the same block antiferromagnetic order as in $K_2Fe_4Se_5$. The Fe order-disorder transition occurs at T_S = 500–578 K, and the antiferromagnetic transition at T_N = 471–559 K with an ordered magnetic moment $\sim 3.3\mu_B$/Fe at 10 K. Thus, all recently discovered A intercalated iron selenide superconductors share the common crystalline and magnetic structure, which are very different from previous families of Fe-based superconductors, and constitute a distinct new 245 family.

DOI: 10.1103/PhysRevLett.107.137003 PACS numbers: 74.25.Ha, 74.70.Xa, 75.25.-j, 75.30.-m

The iron pnictide and chalcogenide superconductors, as exemplified by the ReFeAs(O, F) [1–4], (Ba, K)Fe_2As_2 [5], $Li_{1-x}FeAs$ [6], and $Fe_{1+x}Se$ [7] families of materials, share the Fe square lattice as the common structure feature, which determines the electronic states at the Fermi surfaces responsible for high-T_c superconductivity [8]. The Fe_{1+x}(Se, Te) and $Li_{1-x}FeAs$ have the same crystal structure [9–11], in which the excess Fe and Li deficiency at the same crystallographic site serves to maintain an oxidation state of the Fe ion close to +2. Recently, $K_{0.8}Fe_2Se_2$, regarded as K intercalated FeSe in the $BaFe_2As_2$ structure, has been discovered as a superconductor with T_c above 30 K [12]. Subsequent works replacing K by Rb or Cs [13,14] have led to more new superconductors of T_c up to ~32 K. The heavy departure of Fe from the +2 valency implied by the nominal chemical formulas seem supported by angle-resolved photoemission (ARPES) measurements [15], which would upset the theoretical foundation of the prevailing mechanism of previously discovered Fe-based superconductors [16–19].

However, x-ray and neutron diffraction structure refinement studies have shown that the correct compositions for the A = K or Cs intercalated iron selenide superconductors are close to $A_{0.8}Fe_{1.6}Se_2$ [20,21]. Thus, the new superconductors are not heavily electron doped as previously thought, and Fe has a formal oxidation state close to +2 as in the Fe_{1+x}(Se, Te) superconductors [9,10]. The ~20% Fe vacancies in $K_{0.8}Fe_{1.6}Se_2$ are not randomly distributed in the $BaFe_2As_2$ structure below an order-disordered transition at $T_S \approx 578$ K [21]. Instead, they form an ordered structure with the Fe_1 site almost empty and the Fe_2 site fully occupied in the $\sqrt{5} \times \sqrt{5} \times 1$ supercell as shown in Figs. 1(b) and 1(c) [21]. At a slightly lower temperature, $T_N \approx 559$ K, magnetic moments carried by Fe ions at the Fe_2 site develop a block checkerboard antiferromagnetic order. The Fe vacancy and antiferromagnetic order also drastically alter the topology of the Fermi surface according to band structure calculations [22,23], which would

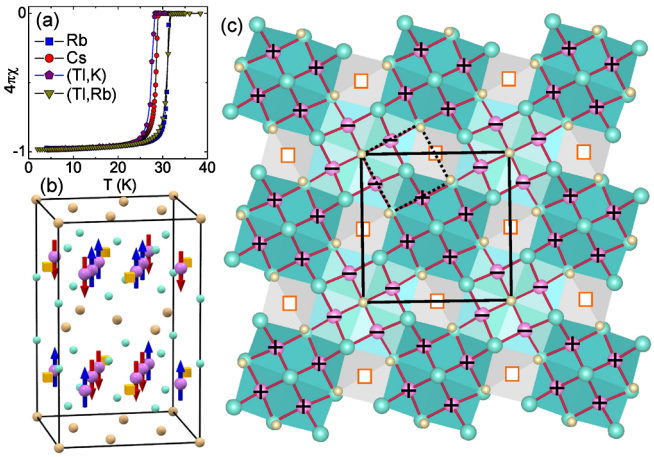

FIG. 1 (color online). (a) Magnetic susceptibility of $A_2Fe_4Se_5$ [A = Rb, Cs, (Tl, K), and (Tl, Rb)] showing the superconducting transition. (b) Common crystal and magnetic structure in the tetragonal $I4/m$ unit cell. The cyan sphere represents Se, the yellow sphere the intercalating A, the orange cube the Fe_1 vacancy site, and the purple sphere the occupied Fe_2 site with a +(−) sign indicating the up(down) magnetic moment along the c axis. There are 4 f.u. per cell. (c) The top Fe-Se layer. The dark and light cyan plaquettes emphasize the four-spin blocks of the up and down spins, respectively, which forms a checkerboard nearest-neighbor antiferromagnetic pattern. From one Fe layer to another, magnetic moments are antiferromagnetically coupled. The solid line denotes the $I4/m$ unit cell, one of the two twins, which breaks the high-temperature symmetry of the $I4/mmm$ unit cell (dashed line) at the Fe order-disorder transition at T_S.

have important physics ramifications and affect the interpretation of the ARPES [15,24,25] and optic [26] data.

Also reported are (Tl, K)Fe_ySe_2 and (Tl, Rb)$Fe_{1.72}Se_2$ superconductors of similarly high $T_c \sim 30$ K [27,28]. What distinguishes these superconductors from the Tl-less ones is the appearance of the superconducting state at the quantum critical point of an antiferromagnetic insulator [27]. It is imperative then to find out whether the K, Cs, or Rb superconductors and the (Tl, K) or (Tl, Rb) superconductors are two different types of new Fe selenide superconductors. We report here a single-crystal neutron diffraction investigation on the Rb, Cs, (Tl, K), and (Tl, Rb) superconductors from about 10 to 580 K that shows the same Fe vacancy and antiferromagnetic order as in the $K_{0.8}Fe_{1.6}Se_2$ superconductor, and the identification of a low T_N in the previous bulk study [27] is incorrect. Hence, superconductivity in all five $A_{0.8}Fe_{1.6}Se_2$ [A = K, Cs, Rb, (Tl, K), and (Tl, Rb)] superconductors develops in a common crystalline and magnetic structure framework, which is distinctly different from the previous Fe square lattice-based families of iron superconductors [1,5–7]. Per chemistry convention, $A_{0.8}Fe_{1.6}Se_2$ is better written as $A_2Fe_4Se_5$ for the new 245 family of superconductors.

Single crystals of $Rb_2Fe_4Se_5$ ($T_c \approx 32$ K) [14], $Cs_2Fe_4Se_5$ ($T_c \approx 29$ K) [29], (Tl, K)$_2Fe_4Se_5$ ($T_c \approx 28$ K) [30], and (Tl, Rb)$_2Fe_4Se_5$ ($T_c \approx 32$ K) [27] superconductors were grown using the Bridgeman method at USTC and ZU, and bulk superconductivity is indicated by the nearly 100% diamagnetic response reported in previous studies using samples grown with the same recipe [14,27,29,30] and shown in Fig. 1(a). A small piece of the $Cs_2Fe_4Se_5$ single crystal from the same batch was used in the previous x-ray crystal structure refinement study at 295 K [20]. Single-crystal neutron diffraction experiments were performed at the High Flux Isotope Reactor of the Oak Ridge National Laboratory. The wide angle neutron diffractometer (WAND) was used to collect Bragg peaks in the $(h0\ell)$, $(2h, h, \ell)$, and $(3h, h, \ell)$ reciprocal planes at various temperatures. The vertically focused Ge(113) monochromator was used to produce a neutron beam of wavelength $\lambda = 1.460$ Å. The curved, one-dimensional ^{3}He position-sensitive detector of 624 anodes covers 125° of the scattering angle. The samples were also investigated using the four-circle diffractometer with neutrons of $\lambda = 1.536$ Å at selected temperatures. The order parameters were measured at WAND for the (Tl, Rb), Cs, and Rb samples, and at the fixed $E_i = 14.7$ meV triple-axis spectrometer HB1A for the (Tl, K) one. The sample temperature was regulated by a high-temperature displex close cycle refrigerator.

In terms of the high temperature $I4/mmm$ unit cell of the $BaFe_2As_2$ structure, the Fe vacancy order is represented by the appearance of the structural superlattice peaks characterized by $\mathbf{Q}_S = (\frac{1}{5}, \frac{3}{5}, 0)$ [20], and the antiferromagnetic order by $\mathbf{Q}_M = (\frac{2}{5}, \frac{1}{5}, 1)$ [21]. Both types of superlattice peaks are accommodated by the $\sqrt{5} \times \sqrt{5} \times 1$ tetragonal $I4/m$ unit cell [21,31] which we use to label reciprocal space in this paper and in which $\mathbf{Q}_S = (110)$ and $\mathbf{Q}_M = (101)$. Figure 2 shows single-crystal diffraction pattern in the $(h0\ell)$ plane at 295 K. Structural Bragg peaks $\{h0\ell\}$ ($h = 2, 4, 6, \ldots$, and $\ell = 0, 2, 4, \ldots$) due to the Fe vacancy order are clearly visible as are magnetic Bragg peaks $\{h0\ell\}$ ($h = 1, 3, 7, \ldots$ and $\ell = 1, 3, 5, \ldots$) caused by the block checkerboard antiferromagnetic order [21]. These "superlattice" peaks are forbidden in the $BaFe_2As_2$ structure.

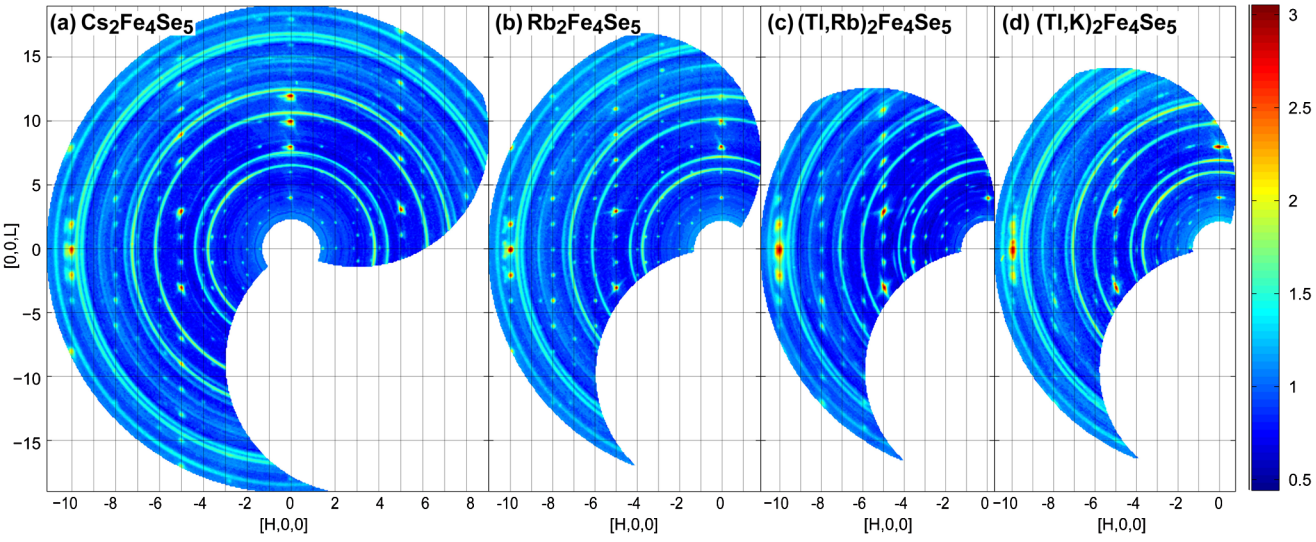

FIG. 2 (color online). Single-crystal neutron diffraction pattern of (a) $Cs_2Fe_4Se_5$, (b) $Rb_2Fe_4Se_5$, (c) (Tl, Rb)$_2Fe_4Se_5$, and (d) (Tl, K)$_2Fe_4Se_5$ measured in the $(h0\ell)$ plane of the $I4/m$ unit cell at $T = 295$ K. In addition to Bragg peaks of the high temperature $I4/mmm$ structure, two new types of contributions to the Bragg reflection appears: (1) structural {200}, {202}, {400}, {402}, etc., caused by the Fe vacancy order, and (2) magnetic {103}, {301}, {303}, {701}, etc., caused by antiferromagnetic order of the Fe moments.

As in previous x-ray and electron single-crystal diffraction studies [20,31,32], twins with the same c-axis exist in all crystals examined in this neutron single-crystal diffraction study. They show up as those superlattice peaks at noninteger h indices in Fig. 2. For example, the $(-1.41, 0, \ell)$ with ℓ even in Fig. 2(a) can be identified as the Fe vacancy peaks (11ℓ) from a twinned domain. During the data reduction, care was paid to resolve the twin distribution. Data collected using WAND and the four-circle diffractometer were consistent with each other. The data analysis was conducted using the FULLPROF program suite. The relative occupancy of Tl and Rb (Tl and K) was fixed by that from the energy dispersive x-ray spectroscopic measurements since our neutron diffraction refinements did not have enough sensibility for an independent determination. Fixing or floating the ratio does not affect appreciably the value of the refined magnetic moment. The total number of independent Bragg reflections used in the refinements were 155, 131, 190, and 132 for the A = Rb, Cs, (Tl, K), and (Tl, Rb) samples, respectively, and the RF factors were 4.8%, 5.6%, 4.5%, and 7.7%, respectively. A summary of the results of the four superconductors investigated in this study is listed in Table I, together with those of $K_2Fe_4Se_5$ from a previous study [21].

Two separated phase transitions due to the antiferromagnetic order and the iron vacancy order have been discovered in a neutron diffraction study on $K_2Fe_4Se_5$ [21], but only the magnetic transition has been reported previously for the Cs compound in a combined μSR and thermometry study [33]. In Fig. 3(a), the integrated intensity of the magnetic Bragg peak (103) and structural Bragg peak (118) of $Cs_2Fe_4Se_5$, simultaneously measured on WAND, is shown as a function of temperature. Similar to the case of the K intercalated superconductor, there are two separated magnetic and structural transitions at $T_N = 471(4)$ K and $T_S = 500(1)$ K, respectively. The order parameters at $\mathbf{Q}_S$ and $\mathbf{Q}_M$ look very similar to those of $K_2Fe_4Se_5$ [21], albeit now that the magnetic and structural transition temperatures of T_N and T_S are lower (Table I and Fig. 3). The T_N reported here agrees with $T_N \approx 477$ K from the previous μSR study [33], which also reports a microscopic coexistence of superconductivity and an unidentified antiferromagnetic order in a nominal $Cs_{0.8}Fe_2Se_{1.96}$ ($T_c \approx 28.5$ K) superconductor. The T_S agrees with that from an x-ray study appearing after we finished the measurement [34]. This is different from previous Fe-based superconductors where an antiferromagnetic order coexisting with superconductivity can be regarded as a relic from the parent antiferromagnet [35]; the antiferromagnetic order in 245 superconductors is very strong. In addition to the high T_N, all the magnetic moments listed in Table I at $\sim$10 K are higher than the previous record $2\mu_B$/Fe found in nonsuperconducting parent compounds [9].

The structural peak at $\mathbf{Q}_S$, which represents the breaking of the high-temperature $I4/mmm$ symmetry when the vacant (orange cube in Fig. 1) and occupied (purple sphere in Fig. 1) Fe sites segregate below T_S, saturates rapidly to its low temperature value [Fig. 3(a)]. Therefore, below the room temperature where relevant physics processes relating to the superconductivity occur, we are dealing with a well-ordered crystal structure in the $I4/m$ symmetry. Structurally, and consequently electronically, using the $BaFe_2As_2$ family of superconductor materials as a model is too remote to the reality. The modification of the electronic structure by the new $I4/m$ crystal symmetry

TABLE I. Physical properties of the $A_2Fe_4Se_5$ superconductors. Lattice parameters at 295 K and the ordered magnetic moment of Fe at 295 K (m) and at $\sim$10 K (M) are listed with T_c, T_N, and Fe vacancy order-disorder transition T_S.

A	K	Rb	Cs	Tl, K	Tl, Rb
a (Å)	8.7306(1)	8.788(5)	8.865(5)	8.645(6)	8.683(5)
c (Å)	14.1128(4)	14.597(2)	15.289(3)	14.061(3)	14.388(5)
m (μ_B)	2.76(8)	2.95(9)	2.9(1)	2.61(9)	2.7(1)
M (μ_B)	3.31(2)	3.3(1)	3.4(2)	3.2(1)	3.2(1)
T_c (K)	32	32	29	28	32
T_N (K)	559(2)	502(2)	471(4)	506(1)	511(1)
T_S (K)	578(2)	515(2)	500(1)	533(2)	512(4)

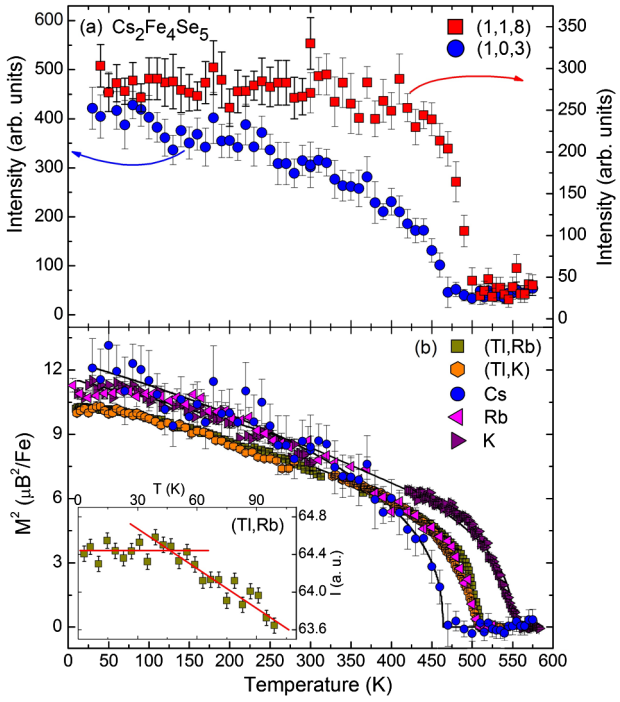

FIG. 3 (color online). (a) Magnetic (103) and structural (118) Bragg peaks vs the temperature, serving as order parameters for the antiferromagnetic and Fe vacancy order-disorder transitions, respectively, in $Cs_2Fe_4Se_5$. (b) Normalized magnetic Bragg intensity representing the squared magnetic moment as a function of the temperature for $A_2Fe_4Se_5$ superconductors. Inset: Magnetic (101) peak of $(Tl, Rb)_2Fe_4Se_5$ showing that its intensity saturates when T_c is approached.

and by the block antiferromagnetic order has been vividly and dramatically demonstrated in first-principle band structure calculations [22,23]. Future investigations on the 245 superconductors should be based on the correct $I4/m$ crystal structure.

When compared to the temperature dependence of the structural peak, the magnetic Bragg peak of $Cs_2Fe_4Se_5$ shows a gradual rise below T_N [Fig. 3(a)], as previously found for $K_2Fe_4Se_5$ [21]. The T_N is lower than T_S, as expected, since the long-range magnetic order builds on the ordered Fe pattern. This is reminiscent of the antiferromagnetic transition in V_2O_3, albeit the underlying transition is to an orbital occupation order [36]. Figure 3(b) illustrates the magnetic order parameters of all five $A_2Fe_2Se_5$ samples with T_N's listed in Table I. As with the K compound, the linear dependence of magnetic Bragg intensity is interrupted by a flat plateau when T_c is approached. For example, the inset of Fig. 3(b) shows a temperature scan measured with much better statistics using a triple-axis spectrometer for the $(Tl, Rb)_2Fe_4Se_5$ sample, suggesting interaction between the antiferromagnetic order and superconductivity as previously discovered in the case of heavy fermion superconductors [37].

Since the discovery of the nominal $K_{0.8}Fe_2Se_2$ superconductor [12], there has been chaotic confusion about the sample composition of the new iron selenide superconductors due to the lack of reliable structure determination work. The Fe-Se square lattice was initially regarded as intact as in the previous families of iron-based superconductors. An analogue to the heavily electron doped iron pnictide superconductors was advocated. Theories based on both the AFe_2Se_2 of the $BaFe_2As_2$ structure and the $AFe_{1.5}Se_2$ of a $\sqrt{2} \times 2\sqrt{2} \times 1$ supercell structure framework were advanced for the new superconductors [16,38]. The superconductivity in the (Tl, K) system appeared to occur at a magnetic quantum critical point [27] and supported a doped Mott insulator scenario [39,40] similar to the case of cuprate superconductors. While electronic properties are indeed very different from previous iron-based superconductors as probed in ARPES [15,24,25], optic [26], NMR [41–43], μSR [33], and Raman scattering [44] studies, an appropriate understanding cannot be achieved without knowing the superconducting composition, crystal structure, and magnetic order determined in neutron and x-ray diffraction structural studies.

In summary, our systematic neutron diffraction works show that K, Cs, Rb, (Tl, Rb), and (Tl, K) intercalated Fe selenide superconductors are members of the common family of the $A_2Fe_4Se_5$ superconductors which share the *same* Fe vacancy and antiferromagnetic order. Not only is the crystal structure of the $A_2Fe_4Se_5$ superconductors in the $\sqrt{5} \times \sqrt{5} \times 1$ $I4/m$ unit cell very different from that in previous iron-based high-T_c superconductors, leading to drastically different Fermi surface topology, the coexistence of superconductivity with the very high T_N and large moment antiferromagnetic order is unprecedented. Although the same Fe ions are involved, given the drastically different crystalline and magnetic structures, the $A_2Fe_4Se_5$ superconductors are unlikely to share the same physics mechanism as in previously discovered families of iron-based superconductors. The future search for new high-T_c superconductors has a wider playground, wich includes a vacancy decorated lattice.

We thank Q. Huang and M. A. Green for useful discussions. The work at RUC, USTC, and ZU was supported by NSFC Grants No. 11034012, No. 10974175, No. 10934005 and by the 973 Program Grants No. 2011CBA00112, No. 2011CBA00103, and No. 2009CB929104. The work at ORNL was supported by the Division of Scientific User Facilities, DOE OBES. WAND is operated jointly by ORNL and JAEA under the U.S.-Japan Cooperative Program in Neutron Scattering.

*wbao@ruc.edu.cn

[1] Y. Kamihara *et al.*, J. Am. Chem. Soc. **130**, 3296 (2008).
[2] X. H. Chen *et al.*, Nature (London) **453**, 761 (2008).
[3] G. F. Chen *et al.*, Phys. Rev. Lett. **100**, 247002 (2008).
[4] Z-.A. Ren *et al.*, Chin. Phys. Lett. **25**, 2215 (2008).
[5] M. Rotter, M. Tegel, and D. Johrendt, Phys. Rev. Lett. **101**, 107006 (2008).
[6] X. Wang *et al.*, Solid State Commun. **148**, 538 (2008).
[7] F.-C. Hsu *et al.*, Proc. Natl. Acad. Sci. U.S.A. **105**, 14262 (2008).
[8] I. I. Mazin *et al.*, Phys. Rev. Lett. **101**, 057003 (2008).
[9] W. Bao *et al.*, Phys. Rev. Lett. **102**, 247001 (2009).
[10] T. M. McQueen *et al.*, Phys. Rev. B **79**, 014522 (2009).
[11] M. J. Pitcher *et al.*, Chem. Commun. (Cambridge) **45**, 5918 (2008).
[12] J. Guo *et al.*, Phys. Rev. B **82**, 180520(R) (2010).
[13] A. Krzton-Maziopa *et al.*, J. Phys. Condens. Matter **23**, 052203 (2011).
[14] A. F. Wang *et al.*, Phys. Rev. B **83**, 060512 (2011).
[15] Y. Zhang *et al.*, Nature Mater. **10**, 273 (2011).
[16] F. Wang *et al.*, Europhys. Lett. **93**, 57003 (2011).
[17] T. A. Maier *et al.*, Phys. Rev. B **83**, 100515(R) (2011).
[18] T. Das and A. V. Balatsky, Phys. Rev. B **84**, 014521 (2011).
[19] I. I. Mazin, Phys. Rev. B **84**, 024529 (2011).
[20] P. Zavalij *et al.*, Phys. Rev. B **83**, 132509 (2011).
[21] W. Bao *et al.*, Chin. Phys. Lett. **28**, 086104 (2011).
[22] C. Cao and J. Dai, Phys. Rev. Lett. **107**, 056401 (2011).
[23] X.-W. Yan *et al.*, Phys. Rev. B **83**, 233205 (2011).
[24] D. Mou *et al.*, Phys. Rev. Lett. **106**, 107001 (2011).
[25] X.-P. Wang *et al.*, Europhys. Lett. **93**, 57001 (2011).
[26] Z. G. Chen *et al.*, Phys. Rev. B **83**, 220507(R) (2011).
[27] M. Fang *et al.*, Europhys. Lett. **94**, 27009 (2011).
[28] H. Wang *et al.*, Europhys. Lett. **93**, 47004 (2011).
[29] J. J. Ying *et al.*, New J. Phys. **13**, 033008 (2011).
[30] R. H. Liu *et al.*, Europhys. Lett. **94**, 27008 (2011).
[31] J. Bacsa *et al.*, Chemical Science **2**, 1054 (2011).
[32] Z. Wang *et al.*, Phys. Rev. B **83**, 140505 (2011).
[33] Z. Shermadini *et al.*, Phys. Rev. Lett. **106**, 117602 (2011).

[34] V. Y. Pomjakushin *et al.*, Phys. Rev. B **83**, 144410 (2011).
[35] H. Chen *et al.*, Europhys. Lett. **85**, 17006 (2009).
[36] W. Bao *et al.*, Phys. Rev. Lett. **78**, 507 (1997).
[37] G. Aeppli *et al.*, Phys. Rev. Lett. **60**, 615 (1988).
[38] X.-W. Yan *et al.*, Phys. Rev. Lett. **106**, 087005 (2011).
[39] C. Cao and J. Dai, Phys. Rev. B **83**, 193104 (2011).
[40] R. Yu, J.-X. Zhu, and Q. Si, Phys. Rev. Lett. **106**, 186401 (2011).
[41] W. Yu *et al.*, Phys. Rev. Lett. **106**, 197001 (2011).
[42] H. Kotegawa *et al.*, J. Phys. Soc. Jpn. **80**, 043708 (2011).
[43] D. A. Torchetti *et al.*, Phys. Rev. B **83**, 104508 (2011).
[44] A. M. Zhang *et al.*, arXiv:1101.2168.